Journal of
Water & Climate Change

IWA PUBLISHING

Journal of Water and Climate Change Vol 14 No 5, 1482 doi: 10.2166/wcc.2023.391

Quantifying the streamflow change and influencing factors with a spatio-temporal coupling analysis framework

Zehui Zhou[a], Lei Yu[b,*], Xiufeng Wu[b], Luchen Zhang[b], Shaoze Luo[b], Yu Zhang[b], Bin Yong[c] and Junqi Sheng[d]

[a] School of Earth Sciences and Engineering, Hohai University, Nanjing 211100, China
[b] State Key Laboratory of Hydrology-Water Resources and Hydraulic Engineering, Nanjing Hydraulic Research Institute, Nanjing 210029, China
[c] State Key Laboratory of Hydrology-Water Resources and Hydraulic Engineering, Hohai University, Nanjing 210098, China
[d] Hangzhou Communication Investment Equipment Technology Development Co. Ltd, Hangzhou, Zhejiang 310051, China
*Corresponding author. E-mail: lyu@nhri.cn

LY, 0000-0002-8609-0566

ABSTRACT

Streamflow change and its influencing factors are synchronous and correlated in temporal and spatial scales. The aim of this study is to develop a spatio-temporal coupling analysis framework for quantifying streamflow change and its influencing factors was established. Specifically, the Mann–Kendall test, Pettitt's test, hierarchical cluster analysis, and Ripley's L-function were jointly used to study the spatial heterogeneity of the temporal evolution of streamflow; and the Soil and Water Assessment Tool (SWAT) model was employed to quantify the impacts of climate and human activities on streamflow change. The preliminary application in the Dawen River Basin (China) case has shown that (1) the natural streamflow change in the basin during 1953–2013 is mainly affected by climate change–human activities, followed by climate change and human activities, accounting for a total area of 52.04, 24.90, and 23.06%, respectively; and (2) the vast majority of sub-basins with relatively large natural streamflow change are mainly driven by climate change (i.e., precipitation). In general, the proposed framework can effectively reflect the spatio-temporal patterns of streamflow change and its influencing factors, which can provide a theoretical basis for water resources management in the context of global change.

Key words: climate change, human activities, spatio-temporal coupling analysis, streamflow change, SWAT model

HIGHLIGHTS

- Developing a spatio-temporal coupling analysis framework for quantifying streamflow and its influencing factors.
- Quantifying the contribution of drivers to the streamflow change on the sub-basin scale.
- Streamflow change and their spatial patterns in the DRB are mainly driven by climate change–human activities.
- The vast majority of sub-basins with relatively large streamflow change are mainly driven by climate change.

GRAPHICAL ABSTRACT

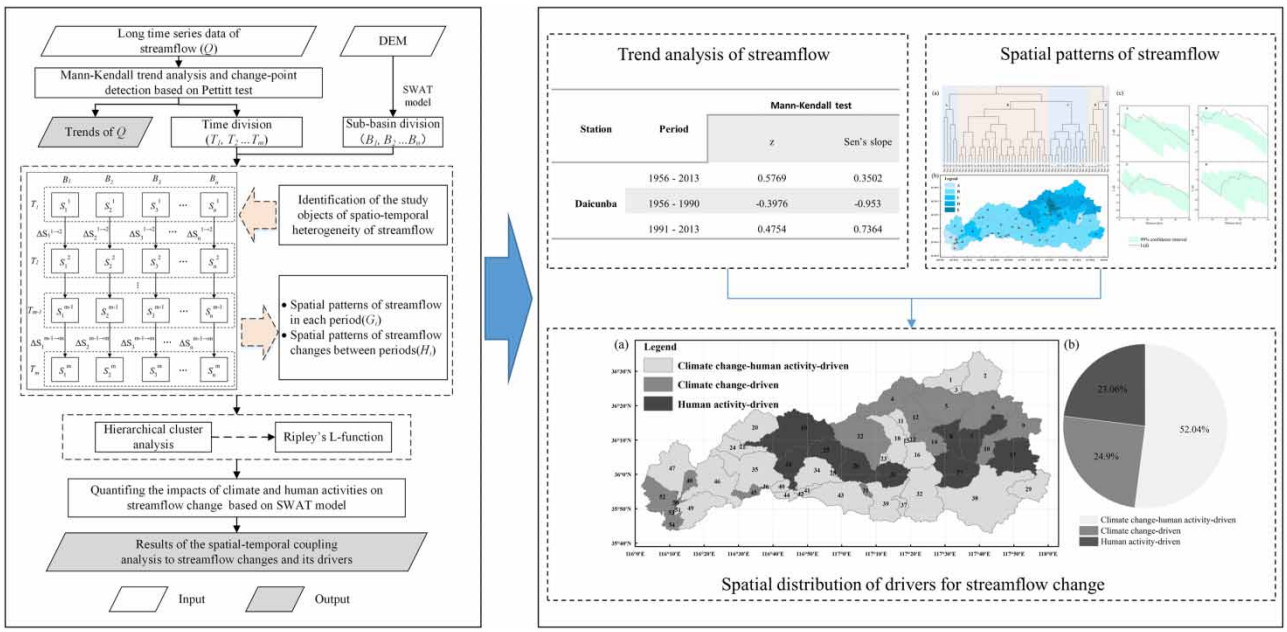

1. INTRODUCTION

In the context of global change (both climate change and human activities), hydrological elements such as streamflow (Dariane & Pouryafar 2021) and evapotranspiration (Wang *et al.* 2021) have exhibited significant variability, causing a variation in the spatio-temporal distributions of water resources, which threatens national or regional water security, energy security, and food security. Therefore, investigating the spatio-temporal characteristics of streamflow change and its influencing factors is the key to successful water resources management, as it helps managers to plan and utilize water resources rationally and improve flood and drought prevention and mitigation capabilities.

Hydrological elements are subject to complex variations, including non-repeatability in temporal terms and non-uniformity in spatial terms (Pan *et al.* 2018). On the one hand, with the development of hydrological observation and the improvement of hydrometeorological data collection, people can obtain long-term time series data about various hydrological elements to study their spatio-temporal patterns following proven time series analysis methods. A variety of analytical methods, including the Mann–Kendall test, Sen's slope estimator, and the Pettitt test, are often utilized jointly to analyze the temporal heterogeneity of hydrometeorological elements. For instance, Bae *et al.* (2008) investigated the spatio-temporal changes of runoff in South Korea from 1968 to 2001 with the Precipitation-Runoff Modelling System, Mann–Kendall's test, regression analysis, and Moran's *I*. They noted that the long-term trend of annual runoff is increasing in the north and decreasing in the southwest. Zhong *et al.* (2021) detected the streamflow trends and their change-points from 1956 to 2017 in the Yellow River Basin (China) using five statistical methods, showing a clear downward trend in streamflow. On the other hand, hydrological elements also have a certain heterogeneity of spatial distribution. At present, the popular analytical methods for studying spatial patterns of hydrological elements are empirical orthogonal function (EOF) and cluster analysis. For example, McCabe & Wolock (2014) classified the stream gauges into 14 clusters based on cluster analysis to increase understanding of the variability of annual mean streamflow from 1951 to 2009 in the conterminous United States. Similarly, Gornik (2020) examined the spatio-temporal variations of streamflow in the Upper Vistula Basin (East-Central Europe) from 1951 to 2015 with Ward's hierarchical cluster analysis. Undeniably, assessing streamflow change is challenging because they interact on temporal and spatial scales and are difficult to disentangle. Unfortunately, in the aforementioned studies, the researchers did not sufficiently consider the synchronization and correlation of spatio-temporal variations for streamflow.

Many attribution methodologies have been developed to detect changes in streamflow, including statistical methods and hydrological models (Zhang *et al.* 2021a). For example, Zhai *et al.* (2016) investigated the spatial and temporal patterns of streamflow and its drivers from 1964 to 2010 in the Lancang River by the Mann–Kendall statistics and dual mass curve

analysis. The results showed that the hydropower plants, land-use/land-cover change (LUCC), and precipitation patterns are the main influencing factors. Li *et al.* (2020) developed a framework to quantify the impacts of climate change and human activities on streamflow based on the SWAT model and Weather Research and Forecasting model in the Yihe River basin (China) from 1951 to 2013. Yang *et al.* (2022) noted that the land surface changes were the dominant factor in river streamflow change in the major river basins of China in recent years based on the Budyko theory. Recently, Li & Quiring (2021) found that the main influencing factors of streamflow change are time-varying rather than constant. This suggests that we need to consider the spatial and temporal characteristics of the influencing factors when conducting attribution analysis of streamflow changes, which is not covered by many current studies.

The paper aims to quantify the streamflow change and its influencing factors from a two-dimensional perspective in space and time with a spatio-temporal coupling analysis framework. Under the framework, the Mann–Kendall test, Sen's slope estimator, Pettitt test, cluster analysis, and Ripley's L-function were linked and used to examine spatio-temporal heterogeneity of streamflow, including the trends of streamflow, spatial patterns of streamflow in different sub-periods, and spatial patterns of streamflow change between sub-periods. The SWAT model was employed to quantify the impacts of climate and human activities on streamflow change. Also, the Dawen River Basin (DRB) was taken as a case study to verify the reasonableness and effectiveness of the proposed framework. This work can provide a theoretical basis for water resources management in the context of global change.

2. METHODS

2.1. Overview of the framework

An overview of the spatio-temporal coupling analysis framework for streamflow change and its influencing factors is presented in Figure 1. The main procedures of the framework are as follows:

Step 1: The Mann–Kendall test is used to reveal the long-term trend in the yearly streamflow (Q); Pettitt's test is employed to detect change-points in the yearly streamflow (Q) and to divide the study period into multiple sub-periods ($T_1, T_2, \ldots, T_m$).

Step 2: The basin is divided into sub-basins based on a digital elevation map (DEM) ($B_1, B_2, \ldots, B_n$).

Step 3: Identification of the study objects of spatio-temporal heterogeneity of streamflow.

The evolutionary characteristics of streamflow at the basin scale are not only reflected in temporal variability, but also in spatial differences. The study objects that need to consider spatio-temporal heterogeneity for the analysis of streamflow variability include two categories: the spatial distribution of streamflow characteristics in each sub-period and the spatial distribution of streamflow variability characteristics between sub-periods. As shown in Figure 1, the streamflow characteristics of the jth sub-basin in the ith sub-period are denoted as S_j^i, and the streamflow variation characteristics of the jth sub-basin between the ith and $(i+1)$th sub-periods are denoted as $\Delta S_j^{i\to i+1}$. Thus, the spatial distribution characteristics of streamflow in the ith sub-period can be denoted by $G_i(S_1^i, S_2^i, S_3^i, \ldots S_n^i)$, and the spatial distribution characteristics of the streamflow variation from the ith sub-period to the $(i+1)$th sub-period can be denoted by $H_i(\Delta S_1^{i\to i+1}, \Delta S_2^{i\to i+1}, \Delta S_3^{i\to i+1}, \ldots, \Delta S_n^{i\to i+1})$. G_i and H_i are the study objects to be considered when studying the spatio-temporal heterogeneity of streamflow at a basin scale.

Step 4: Hierarchical cluster analysis and Ripley's L-function are employed to evaluate the spatial heterogeneity of the temporal evolution of streamflow.

We first use the hierarchical cluster method to cluster n sub-basins and obtain several clusters with different streamflow characteristics, where each cluster contains several sub-basins with similar streamflow characteristics. Each sub-basin is then generalized to a point so that the problem of the spatial distribution of streamflow in the basin can be abstracted as a point pattern problem. Finally, Ripley's L-function is employed to analyze the spatial distribution pattern of each cluster, specifically: the corresponding L-value is calculated by selecting the distance scales according to the basin area, and the simulated $L(d)$ Monte Carlo curve is plotted with the actual $L(d)$ curve so that the spatial distribution of each cluster can be identified.

Step 5: The SWAT model is employed to quantify the impacts of climate and human activities on streamflow change at spatial and temporal scales.

2.2. Reconstructing natural streamflow and attribution analysis of streamflow change based on the SWAT model

The SWAT model, a physically based, continuous-time, and semi-distributed hydrological model developed by the United States Department of Agriculture (USDA) Agricultural Research Service, can predict the water movement in complex

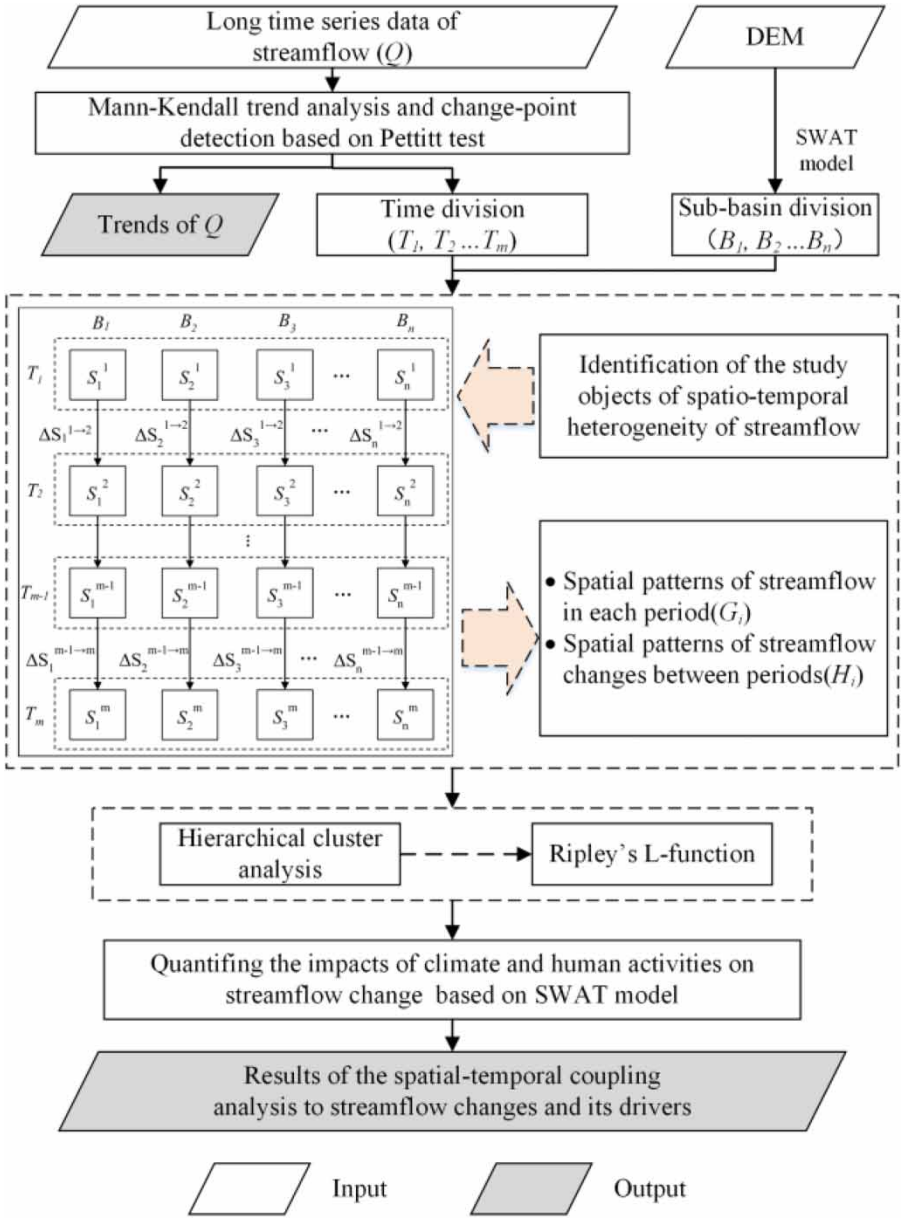

Figure 1 | Framework for spatio-temporal coupling analysis to streamflow change and its influencing factors.

basins with varying soils, land use, and management conditions over long-term periods (Li *et al.* 2019). In this study, we used the SWAT model to reconstruct natural streamflow in the study area. First, the meteorological data such as precipitation and temperature for the same period are used as model inputs. Then, sub-basins in the basin that are less affected by human activities are selected for model calibration, and the rationality is verified by the observed data. Finally, the natural streamflow of each sub-basin is calculated by the model.

Also, the Fixing-Changing method based on the SWAT model was used for the attribution analysis streamflow change at spatial and temporal scales. The total streamflow change between the ith and $(i+1)$th sub-periods in the jth sub-basin (ΔS_j^i) is as follows:

$$\Delta S_j^i = S_j^{i+1} - S_j^i, \quad i = 1, 2, \ldots, m-1; j = 1, 2, \ldots, n \tag{1}$$

where S_j^{i+1} and S_j^i refer to the simulated streamflow of jth sub-basin by the SWAT model in the ith and $(i+1)$th sub-periods, respectively.

When climate factors are given only as variables:

$$\Delta S_{C,j}^i = S_{C,j}^{i+1} - S_{C,j}^i, \quad i = 1, 2, \ldots, m-1; j = 1, 2, \ldots, n \tag{2}$$

where $\Delta S_{C,j}^i$ is the streamflow change caused by the climate change between the ith and $(i+1)$th sub-periods in the jth sub-basin; $S_{C,j}^{i+1}$ and $S_{C,j}^i$ refer to the simulated streamflow of jth sub-basin in the ith and $(i+1)$th sub-periods, respectively.

When human activities factors are given only as variables:

$$\Delta S_{H,j}^i = S_{H,j}^{i+1} - S_{H,j}^i, \quad i = 1, 2, \ldots, m-1; j = 1, 2, \ldots, n \tag{3}$$

where $\Delta S_{H,j}^i$ is the streamflow change caused by the human activities between the ith and $(i+1)$th sub-periods in the jth sub-basin; $S_{H,j}^{i+1}$ and $S_{H,j}^i$ refer to the simulated streamflow of the jth sub-basin in the ith and $(i+1)$th sub-periods, respectively.

Furthermore, we performed cluster analysis on the results attribution analysis. The number of streamflow evolution types for each sub-basin clustered according to the ΔS_j^i value is *Num*, the number of streamflow evolution types for each sub-basin clustered according to the $\Delta S_{C,j}^i$ value is *NumC*, and the number of streamflow evolution types for each sub-basin clustered according to the $\Delta S_{H,j}^i$ value is *NumL*. The dominant influencing factor is determined according to the following equation:

$$\theta_j^i = |NumC_j^i - Num_j^i| - |NumL_j^i - Num_j^i| \tag{4}$$

where θ_j^i is the indicator variable of the dominant factor of streamflow change between the ith and $(i+1)$th sub-periods in the jth sub-basin. If $\theta_j^i < 0$, it indicates that the dominant factor of streamflow change in the jth sub-basin is climate change; if $\theta_j^i > 0$, it indicates that the dominant factor of streamflow change in the jth sub-basin is human activities; if $\theta_j^i = 0$, it indicates that the streamflow change in the jth sub-basin is jointly dominated by climate change and human activities.

2.3. Trend analysis and change-point detection

The Mann–Kendall test, Sen's slope estimator, and Pettitt test are usually linked and used when detecting trends and change-points of hydrometeorological variables, including streamflow, precipitation, and potential evapotranspiration (Meng *et al.* 2019). The Mann–Kendal test, which was proposed by Mann and Kendall, was employed to ascertain the trends of streamflow at key stations over the study area (at a significance level of $P \leq 0.05$), with the magnitudes of the trends characterized using Sen's slope. The Pettitt test, which was proposed by Pettitt, was used to detect the change-point with a significance test (at a significance level of $P \leq 0.05$). The results provide a reasonable division of the period, which is crucial for the spatio-temporal coupling analysis.

2.4. Hierarchical cluster analysis

Cluster analysis is an unsupervised multivariate technique for characterizing the grouping structure of specific datasets (Yang *et al.* 2019). The hierarchical clustering method is one of the most commonly used cluster analysis methods, which is simple, intuitive, and easy to interpret, and is widely used in hydrology and ecology (Gornik 2020). Therefore, we choose the method to cluster the sub-basins to describe the spatial variability of streamflow in terms of clusters and determine the spatial distribution pattern of each cluster with different streamflow characteristics separately.

The principle of this method is to consider the sub-basin as the smallest cluster and calculate the distance between clusters, then merge the two clusters with the shortest distance into a new cluster; then calculate the distance between the new, and remaining, clusters, and merge the two clusters with the shortest distance into a new cluster again, and so on, until they are merged into one large cluster (Supplementary Figure S1).

When clustering sub-basins according to streamflow characteristics, the longest distance method is used to calculate the distance (Euclidean distance) between clusters:

$$D_{ab} = \max(d_{ij}), \quad X_i \in Y_a;\ X_j \in Y_b \tag{5}$$

where X_i and X_j denote the ith and jth sub-basins, which belong to the cluster Y_a and cluster Y_b, respectively; d_{ij} is the Euclidean distance between X_i and X_j.

2.5. Ripley's L-function

Ripley's L-function method is a distance-based point pattern analysis method, which is often used to portray spatial clustering across different scales (Wilschut *et al.* 2015). In this study, each sub-basin is generalized to a point (i.e., the centroid), so the problem of the spatial pattern of streamflow can be abstracted as a point pattern problem. Therefore, Ripley's L-function method is chosen here to examine the spatial clustering of various sub-basins. The details are as follows:

$$K(d) = \frac{A}{n^2}\sum_{i=1}^{n}\sum_{\substack{j=1 \\ j \neq i}}^{n}\delta_{ij}(d) \tag{6}$$

$$\delta_{ij}(d) = \begin{cases} 1, & d_{ij} \leq d \\ 0, & d_{ij} > d \end{cases} \tag{7}$$

and Ripley's L-function is given by the following equation:

$$L(d) = \sqrt{K(d)/\pi} - d \tag{8}$$

where d is the distance; A is the area of the study area containing all points; n represents the number of all points; $\delta_{ij}(d)$ is the indicator function, see Equation (3). d_{ij} denotes the Euclidean distance between point i and point j.

In practical applications, the simulated $L(d)$ curve obtained from the random distribution was plotted in the same coordinate system as the actual $L(d)$ curve, and the type of spatial distribution was judged by the relationship between the positions of the curves. In the present study, the Monte Carlo method was used to solve the upper and lower envelope (99% confidence interval) of the random distribution and the judgment criteria are as follows (Lancaster & Downes 2004): if the actual L-value of the point events lies above the upper envelope, the point events are aggregated in space; if the actual L-value of the point events lies between the upper and lower envelopes, the point events are randomly distributed in space; and if the actual L-value of the point events lies below the lower envelope, the point events are regularly dispersed in space.

3. STUDY AREA AND DATA

3.1. Study area

The DRB was chosen as the case study area to reveal its spatio-temporal characteristics of streamflow with the proposed framework. The Dawen River is the largest tributary of the lower reaches of the Yellow River, with a total length of 239 km and a drainage area of 9,069 km^2, between 116° and 118°E and 35.7° and 36.6°E (Figure 2). It has a semi-humid climate with a mean annual temperature of 12.6 °C and a mean annual precipitation of 711.1 mm. Precipitation varies greatly from year-to-year and is unevenly distributed within the year, while there are large geographical differences, with more precipitation in the mountains than in the plains and more precipitation in the east than in the west. In addition, water and drought disasters occur occasionally, adversely restricting the healthy and rapid development of the region's economy and society. In general, the streamflow characteristics of the DRB have significant spatio-temporal variability due to various influences such as climate, topography, and human activities.

3.2. Data

Daily streamflow data from five hydrological stations (Figure 2, see Supplementary Table S1 for more details) and daily precipitation data of 57 meteorological stations from 1968 to 2013 were collected from the China Annual Hydrological Reports. The local DEM was derived from the Shuttle Radar Topography Mission (SRTM) dataset with a resolution of 30 m. Land-cover maps from 1990 to 2000 were obtained from https://www.resdc.cn. The soil types in the DRB were derived from the Harmonized World Soil Database (HWSD) with a resolution of 1 km (https://www.fao.org).

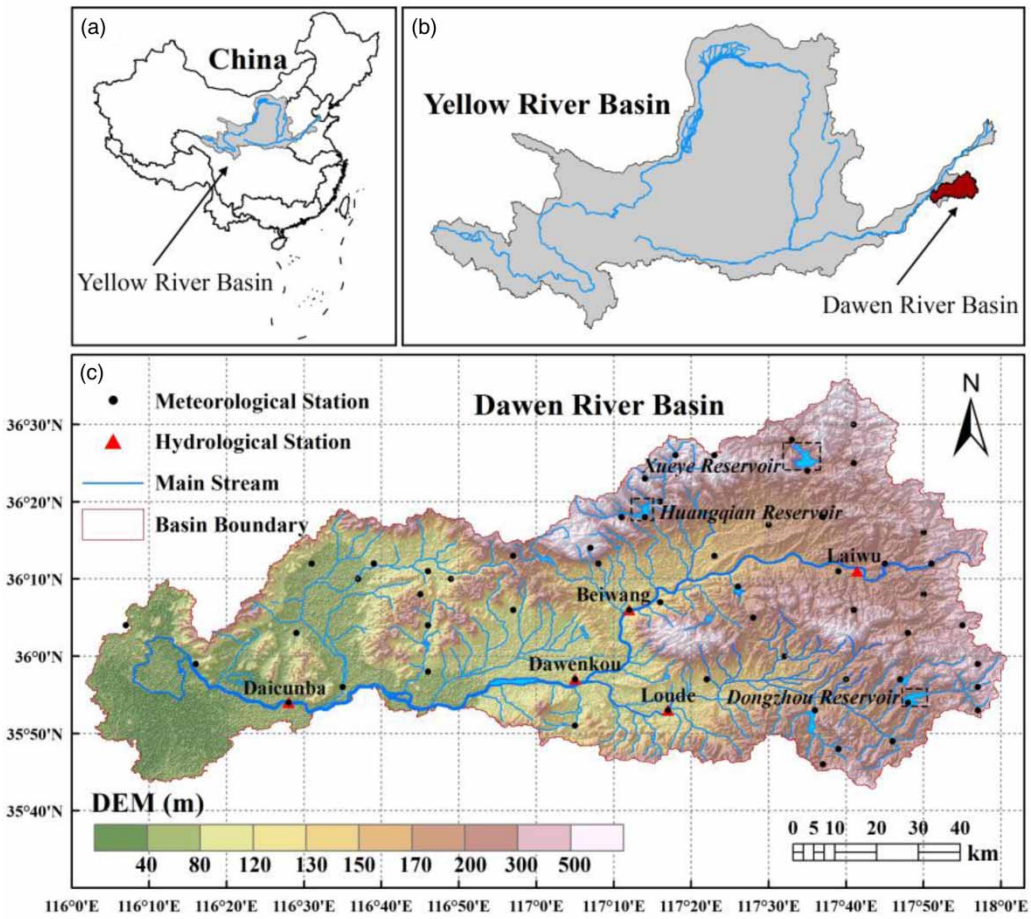

Figure 2 | Study area.

4. RESULTS AND DISCUSSION

As an important component of water resource management, detailed characterization to reveal the spatio-temporal evolution of natural streamflow is the key to a success for adaptive water resources management and a prerequisite for sustainable water resources utilization. Thus, this study took the natural streamflow as the research object and conducted the spatio-temporal evolution analysis of streamflow, aiming to provide a theoretical basis for water resources management in the basin. The SWAT model was employed to reconstruct the natural streamflow of the DRB, and the calibration and validation were described in the Supplementary Information. Evidently, the SWAT model has high precision of the streamflow simulation in the DRB, with all R^2 greater than 0.9. Meanwhile, the DRB was divided into 54 sub-basins with coding by the SWAT model, as shown in Supplementary Figure S2. Here, we used the proposed framework to study the spatio-temporal heterogeneity of natural streamflow change and its influencing factors in the DRB, specifically including long-term trend and change in natural streamflow and spatial heterogeneity in the temporal evolution of natural streamflow.

4.1. Long-term trend and change in natural streamflow

The Pettit test was adopted to detect the change-point of natural streamflow at Daicunba station from 1956 to 2013 which is the key station of DRB with a controlling area of 91.12% of the basin. According to the results, 1990 was the change-point with $P = 0.8870$ (at a significant level of $P > 0.05$), which indicated that the test was statistically insignificant. According to Zhong *et al.* (2021), the turning point of the streamflow in the lower Yellow River Basin from 1956 to 2017 occurred in 1990 following five statistical methods, including Mann–Whitney *U*-test, Moving *t*-test, Mann–Kendall test, Ordered cluster analysis, and Pettitt test. Therefore, the study period (1956–2013) was derived into two sub-periods by 1990: the early period (1956–1990) and the recent period (1991–2013).

Table 1 | Trend analysis of the natural streamflow for five stations (1956–2013)

Station	Period	Mann–Kendall test	
		z	Sen's slope
Laiwu	1956–2013	0.1476	0.1473
	1956–1990	−1.1077	−1.9234
	1991–2013	0.9508	3.7093
Beiwang	1956–2013	0.5232	0.5324
	1956–1990	−1.0225	−1.4709
	1991–2013	1.1621	4.1584
Loude	1956–2013	0.1476	0.1029
	1956–1990	−0.5965	−1.6247
	1991–2013	0.6867	3.2716
Dawenkou	1956–2013	0.7781	0.6489
	1956–1990	−0.5397	−1.229
	1991–2013	1.1621	2.7209
Daicunba	1956–2013	0.5769	0.3502
	1956–1990	−0.3976	−0.953
	1991–2013	0.4754	0.7364

Table 1 lists the results of the analysis of natural streamflow trends at the five hydrological stations, and it can be seen that all stations show an increasing trend throughout the entire study period (1956–2013), and a decreasing trend in the early period (1956–1990), and an increasing trend in the recent period (1991–2013). In addition, the magnitude of streamflow change during the recent period at the four stations (except for the Daicunba) is greater than that in the early period, which may be related to the extent of climate change during the recent period compared with that in the early period (Johnson *et al.* 2020). However, the changes in the trend in the three periods at all stations are not statistically significant (at $P > 0.05$), which is mainly because this study restores the observed streamflow to natural streamflow and weakens the effects of human activities.

4.2. Spatial heterogeneity of temporal evolution of natural streamflow

In this study, we took the average streamflow of three periods in the DRB as an example to study its spatial pattern and verify the feasibility of the proposed framework. Here, the average values of natural streamflow from 1956 to 1990 under the underlying surface in 1990 were calculated as the result of natural streamflow during the early period and the average values of streamflow from 1991 to 2013 under the underlying surface in 2010 were derived as the result of natural streamflow during the recent period for the 54 sub-basins in the DRB. The spatial heterogeneity of the temporal evolution of natural streamflow was studied in terms of the spatial pattern of natural streamflow in early and recent periods, and the spatial patterns of streamflow change from the early to the recent period.

4.2.1. Spatial patterns of natural streamflow in the early period

Figure 3(a) illustrates the clustering map of sub-basins under natural streamflow in the early period in the DRB, according to which all sub-basins are divided into five clusters based on streamflow, namely, I, II, III, IV, and V, demonstrating very small streamflow, small streamflow, moderate streamflow, large streamflow, and very large streamflow, respectively. The spatial distribution of natural streamflow for sub-basins is shown in Figure 3(b): the numbers therein are the sub-basin numbers. It can be seen that Cluster I (very small streamflow) contains a small number of sub-basins, mainly located in the southern area of the middle DRB; sub-basins included in Cluster II with small streamflow are mainly concentrated in the lower DRB; sub-basins included in Cluster III with moderate streamflow are widely distributed throughout the basin; sub-basins included in Cluster IV with large streamflow are distributed across a wide area in the upper DRB and a few areas in the lower DRB; sub-basins included in Cluster V with very large streamflow are concentrated in the upper, and localized areas in the middle, areas of the basin.

The L-functions for clusters I–V in the early period are shown in Figure 3(c), and the distance scales studied are from 0 to 50 km. Based on the positional relationship between the simulated $L(d)$ curve with a 99% confidence interval by the Monte

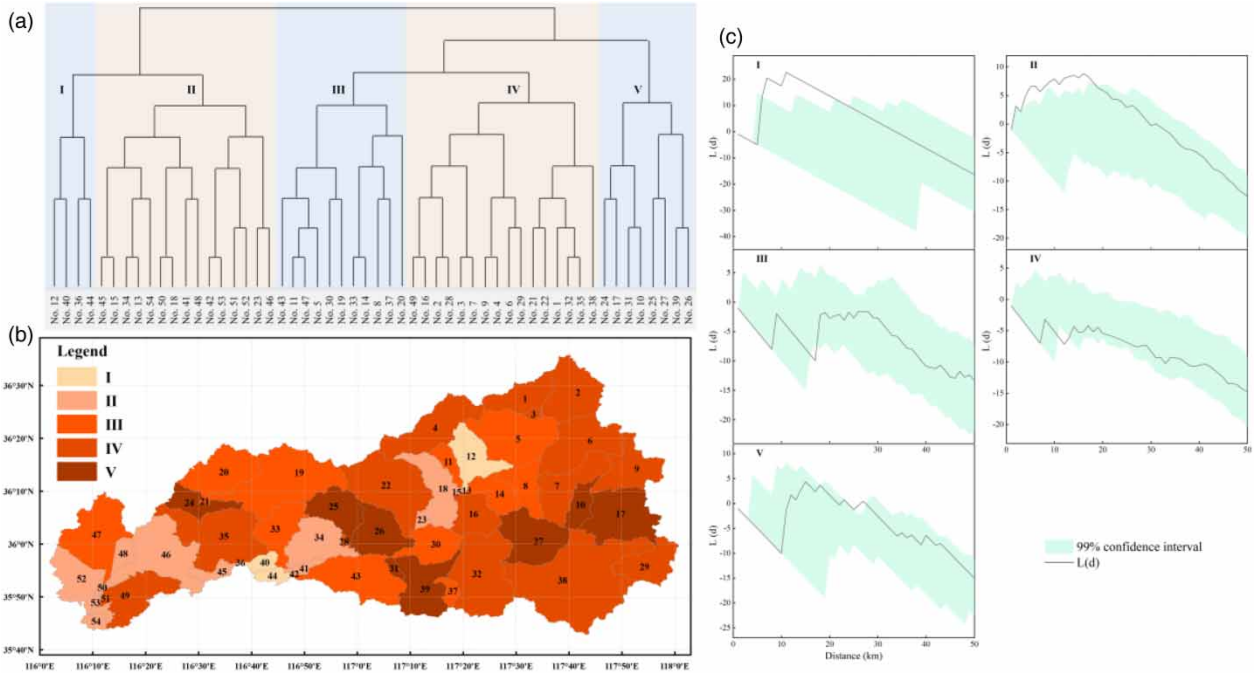

Figure 3 | Spatial patterns of natural streamflow in the early period in the DRB: (a) clustering map of sub-basins, (b) spatial distribution, and (c) L-functions for clusters I–V. (Note: Clusters I, II, III, IV, and V demonstrate very small streamflow, small streamflow, moderate streamflow, large streamflow, and very large streamflow, respectively.)

Carlo method and the actual $L(d)$ curve, we find that sub-basins included in Cluster I with very small streamflow have an aggregated distribution at distances $6 \leq d \leq 21$ km and a random distribution at the rest of the distances; sub-basins included in Cluster II with small streamflow have an aggregated distribution at $3 \leq d \leq 18$ km and a random distribution at the rest of the distances; sub-basins included in Cluster III with moderate streamflow have a uniform distribution at $16 \leq d \leq 17.5$ km and a random distribution at the rest of the distances; sub-basins included in Cluster IV with large streamflow are uniformly distributed at $10.5 \leq d \leq 13$ km and randomly distributed at the rest of the distances; Cluster V with very large streamflow are aggregated at $25 \leq d \leq 27.5$ km and randomly distributed at the rest of the distances. Overall, Clusters I and II show aggregation at intermediate distances, and Clusters III, IV, and V show aggregation at small distances.

4.2.2. Spatial patterns of natural streamflow in the recent period

Figure 4(a) illustrates the clustering map of sub-basins under natural streamflow in the recent period in the DRB, according to which all sub-basins are divided into four clusters based on streamflow sizes, namely, i, ii, iii, and iv, indicating very small streamflow, small streamflow, large streamflow, and very large streamflow, respectively. The spatial distribution of natural streamflow for sub-basins is shown in Figure 4(b). It is found that sub-basins included in Clusters i (very small streamflow) and ii (small streamflow) are concentrated in the middle and lower DRB; sub-basins included in Cluster iii with large streamflow are distributed across all areas of the basin, with the majority in the upper DRB; sub-basins included in Cluster iv with very large streamflow are mainly located in the upper and middle DRB.

The L-functions for clusters i–iv in the recent period are illustrated in Figure 4(c): sub-basins included in Cluster i with very small streamflow have an aggregated distribution at $3.5 \leq d \leq 31$ km and a random distribution at the rest of the distances; the sub-basins included in Cluster ii with small streamflow have a uniform distribution at $10.5 \leq d \leq 13$ km and a random distribution at the rest of the distances; the sub-basins included in Clusters iii (large streamflow) and iv (very large streamflow) are randomly distributed across all distances. In summary, Cluster i shows aggregation on large distances, Cluster ii shows aggregation on small distances, and Clusters iii and iv do not show aggregation.

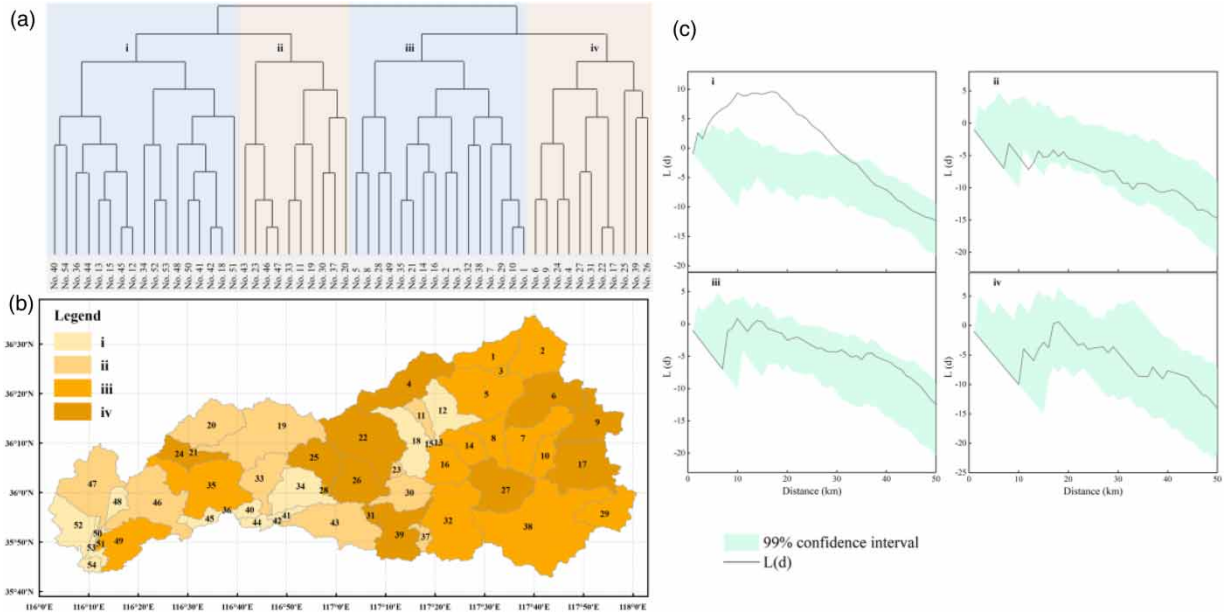

Figure 4 | Spatial patterns of natural streamflow in the recent period in the DRB: (a) clustering map of sub-basins, (b) spatial distribution, and (c) L-functions for clusters i–iv. (Note: Clusters i, ii, iii, and iv indicate very small streamflow, small streamflow, large streamflow, and very large streamflow, respectively.)

4.2.3. Spatial patterns of natural streamflow change from the early to recent periods

Figure 5(a) shows the clustering map of sub-basins under natural streamflow change from the early to recent periods in the DRB, according to which all sub-basins are divided into five clusters based on the degree of streamflow change, namely, A, B, C, D, and E, indicating a large decrease in streamflow, a very small change in streamflow, a small increase in streamflow, a larger increase in streamflow, and a very large increase in streamflow, respectively. The spatial distribution of natural streamflow change for sub-basins is demonstrated in Figure 5(b), which shows that Cluster A (a large decrease in streamflow) contains a small number of sub-basins, accounting for only 3.71% of the total area, mainly located in the westernmost area of the lower DRB; Cluster B (a very small change in streamflow) contains a large number of sub-basins and is widely distributed throughout the basin, accounting for 55.94% of the total area; sub-basins included in Cluster C (a smaller increase in streamflow) mainly located in the northern area of the upper DRB, covering 20.58% of the total area; Cluster D (a large increase in streamflow) contains a small number of sub-basins, representing 17.89% of the total area, mainly located in the northern area of the upper DRB; Cluster E (a very large increase in streamflow) has only one sub-basin (No. 12) with only 20.58% of the area.

The L-functions for clusters A–D from the early to recent periods are illustrated in Figure 5(c): the sub-basins with a large decrease in streamflow (Cluster A) show an aggregated distribution at $16 \leq d \leq 19$ km and a random distribution across other distances; the sub-basins with a very small change (Cluster B) in streamflow show an aggregated distribution at $13.5 \leq d \leq 23.5$ and $24.5 \leq d \leq 50$ km and a random distribution across other distances; the sub-basins with a small increase in streamflow (Cluster C) have an aggregated distribution at $33 \leq d \leq 41$ km and a random distribution across other distances; the sub-basins with a large increase in streamflow (Cluster D) have a random distribution across all distances. Thus, the natural streamflow in the DRB showed a smaller degree of variability during 1953–2013 (Clusters B and C), with some clustering. Precipitation is one of the key factors in determining the spatial pattern of streamflow change, so we mapped the spatial distribution of precipitation change from the early to recent periods in the DRB (Figure 6). It can be seen that the precipitation has a large decrease in the plains of the lower DRB, which accounts for a large decrease in streamflow in the area (Cluster A). Also, the precipitation has a very large increase in the No. 12 sub-basin, which accounts for the very large increase in streamflow in the sub-basin (Cluster E).

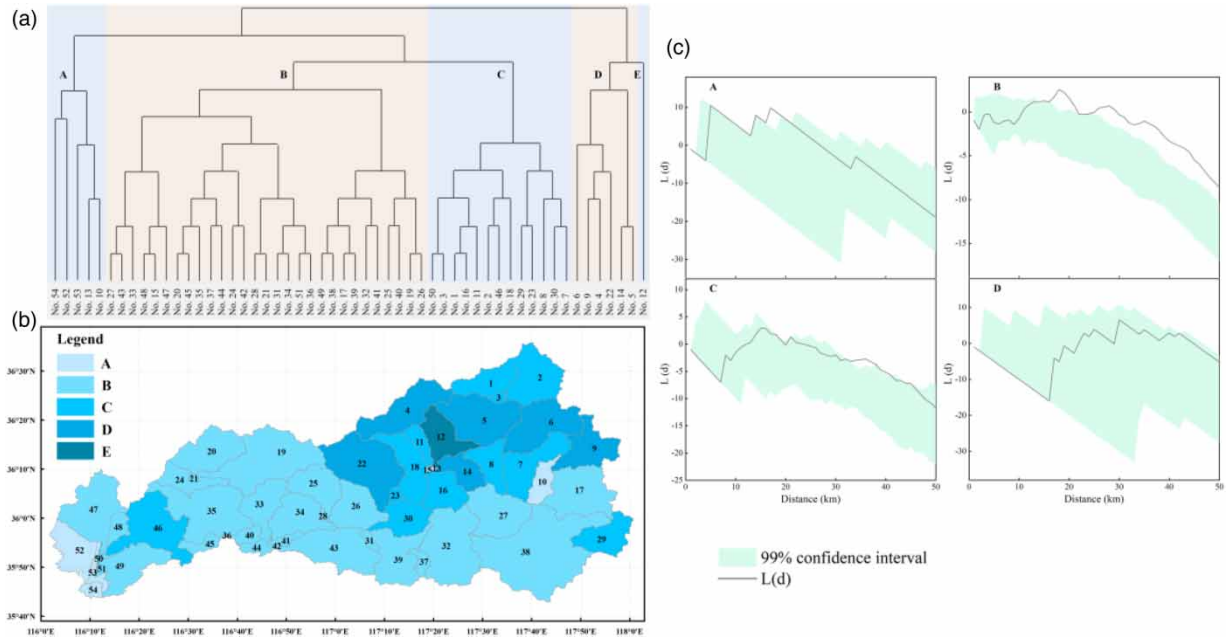

Figure 5 | Spatial patterns of natural streamflow change from the early to recent periods in the DRB: (a) clustering map of sub-basins, (b) spatial distribution, and (c) L-functions for clusters A–E. (Note: Clusters A, B, C, D, and E indicate a large decrease in streamflow, a very small change in streamflow, a small increase in streamflow, a larger increase in streamflow, and a very large increase in streamflow, respectively.)

4.3. Influences of climate change and human activities on streamflow change

Many studies have shown that streamflow change is mainly driven by climate change and human activities (Dey & Mishra 2017; Zhang *et al.* 2020). On the one hand, the key climatic influencing factors affecting streamflow are precipitation and temperature, with the former being the most important. On the other hand, the effects of human activities can be divided into two categories: (1) direct human influences, mainly water withdrawal from rivers and reservoir storage and discharge; and (2) indirect human influences, mainly LUCC (Ma *et al.* 2010). Accordingly, natural streamflow change is mainly driven by precipitation (climate change) and LUCC (human activities) (Yuan *et al.* 2018).

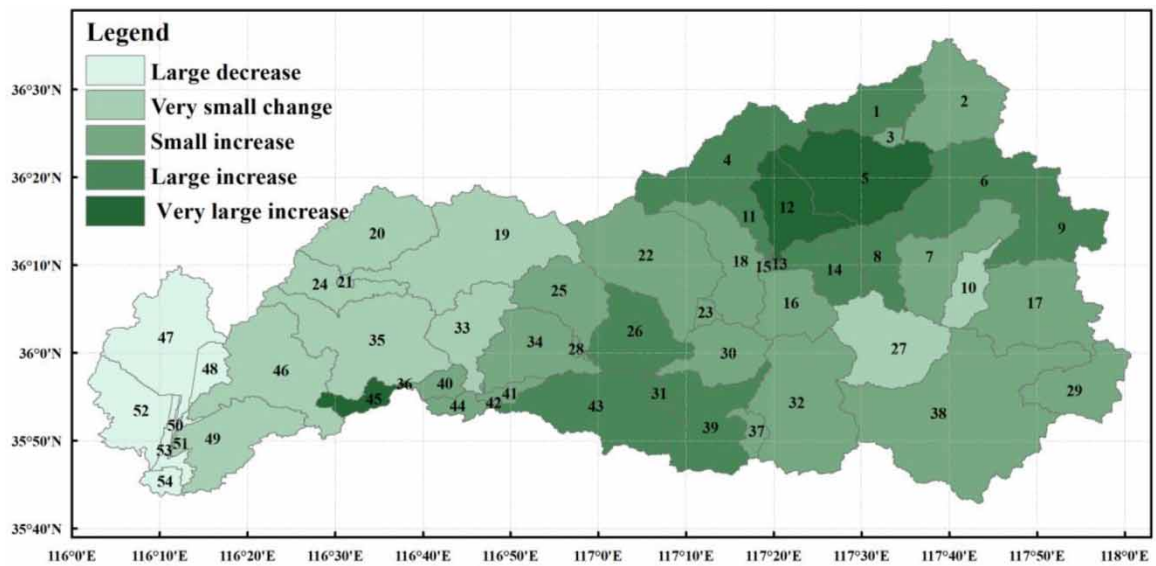

Figure 6 | Spatial distribution of precipitation change from the early to recent periods in the DRB.

Cluster analysis was used to elucidate the spatial patterns of natural streamflow and its influencing factors (precipitation and LUCC), whereupon these three can be considered as categorical variables. Therefore, we employed the chi-squared test, a non-parametric test for categorical variables, with the number of sub-basins as the sampling frequency, to perform the correlation analysis of the three (i.e., natural streamflow, precipitation (climate change), and LUCC (human activities)) (Supplementary Table S2). The result shows that the significance levels of the test subjects with correlations are all below 10%, and the minimum can fall below 0.5%, which means that there is a significant correlation between the spatio-temporal distribution of natural streamflow and precipitation and LUCC in the DRB. This result further verifies that natural streamflow variability is mainly driven by precipitation and LUCC, which is also consistent with the findings of Yuan *et al.* (2018) and Ma *et al.* (2010).

Here, we divided the dominant influences on streamflow change into three categories based on the results of the chi-squared test: climate change (CC), human activity (HA), and climate change–human activity (CC-HA). Figure 7 shows the spatial distribution of influencing factors for natural streamflow change from the early to recent periods in the DRB. It can be seen that 15 sub-basins are driven by CC, accounting for 24.90% of the total area; 10 sub-basins are driven by HA, accounting for 23.06% of the total area; 29 sub-basins are driven by CC-HA, accounting for 52.04% of the basin area. Furthermore, we analyzed the attribution of different degrees of natural streamflow change in the DRB, using the area as the metric (Table 2). The vast majority of sub-basins with relatively large streamflow change (Clusters A, D, and E) are mainly driven by CC; the most of sub-basins with small streamflow changes (Clusters B and C) are driven by CC-HA. One of the reasons is that the study subject considered in this study is natural streamflow, which reduces the direct influence of human activities such as water extraction to some extent.

To explore the direct impacts of human activities on streamflow change, the Daicunba hydrological station (the control station of the DRB) was taken as an example to compare and analyze the differences between its natural and observed streamflow (Figure 8). The observed streamflow at this station is shown to be smaller than the natural streamflow, indicating that the direct influences of human activities such as water withdrawal from rivers and reservoir storage and discharge contribute negatively to the streamflow change, which is consistent with those from previous studies in the Yellow River Basin (Wang *et al.* 2020;

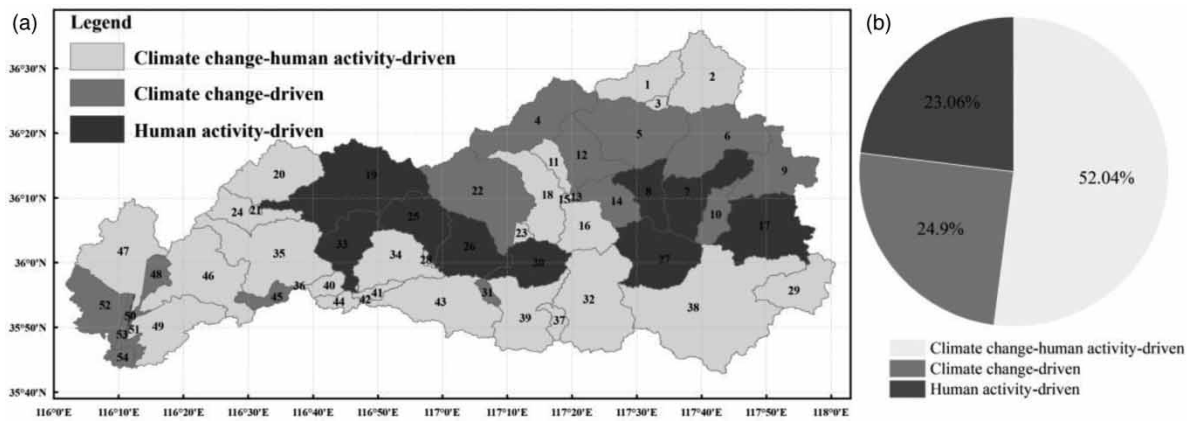

Figure 7 | Spatial distribution of influencing factors for natural streamflow change from the early to recent periods in the DRB.

Table 2 | Attribution analysis for different degrees of streamflow change (Clusters A–E) from the early to recent periods in the DRB

Degree of streamflow change	Climate change–human activity (CC-HA)	Climate change (CC)	Human activity (HA)
A large decrease in streamflow (Cluster A)	0.83%	99.17%	0
A very small change in streamflow (Cluster B)	66.35	2.58%	31.07%
A small increase in streamflow (Cluster C)	72.37%	0	27.63%
A larger increase in streamflow (Cluster D)	0	100%	0
A very large increase in streamflow (Cluster E)	0	100%	0

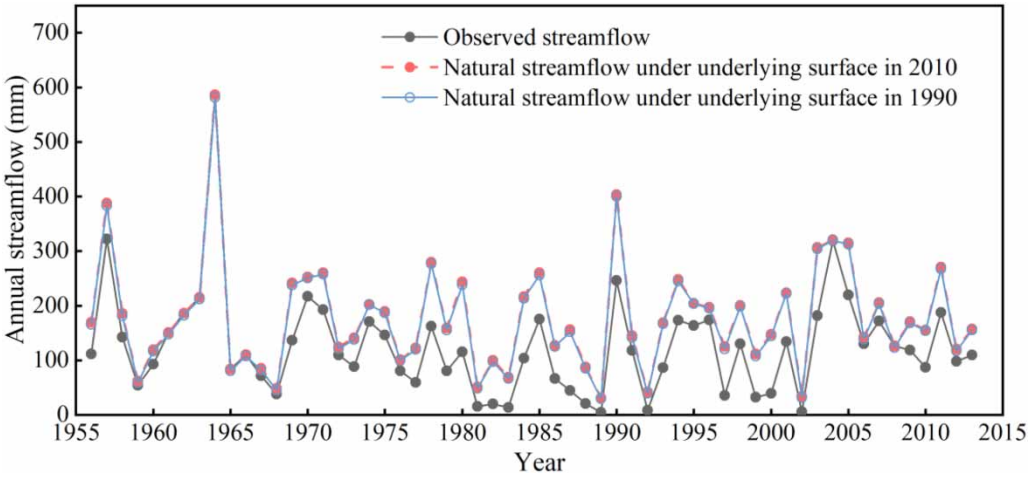

Figure 8 | Observed and natural streamflow at Daicunba hydrological stations from 1956 to 2013.

Zhong *et al.* 2021). Additionally, the results show that the natural streamflow simulated by the SWAT model under the underlying surface in 1990 is the same as in 2010, indicating that the underlying surface changes do not significantly affect the streamflow in the DRB. Therefore, streamflow change in the basin is mainly impacted directly by human activities (e.g., water withdrawal from rivers and reservoir storage and discharge), while the indirect effect (LUCC) is relatively small.

4.4. Implications of the spatio-temporal coupling analysis framework

Some studies demonstrated the temporal variations of streamflow by taking the basin as an entire (i.e., at the basin outlet cross-section) or dividing it into limited sub-basins according to upstream and downstream regions thereof, ignoring the streamflow characteristics within the basin (Yuan *et al.* 2018; Zhong *et al.* 2021), however, we found that streamflow change in the sub-basins of the DRB was inconsistent, with increases and decreases therein (Figure 5(b)). Meanwhile, some researchers focused on spatial patterns of streamflow in the same period, failing to reveal the evolution of streamflow spatial patterns over time (McCabe & Wolock 2014; Gornik 2020). Nevertheless, we found that the spatial patterns of streamflow vary with time (Figures 3(b) and 4(b)). Furthermore, the streamflow change may be superimposed or offset between sub-basins: streamflow change in the sub-basins are insignificant, but the superimposed effect is due to the inconsistent direction of streamflow in each sub-basin, resulting in the change of streamflow at the basin outlet section being significant; streamflow change in the sub-basins are significant, but the offsetting effect is due to the inconsistent direction of streamflow in each sub-basin, resulting in the change of streamflow at the basin outlet section being insignificant (a detail the likes of which the aforementioned studies could not capture).

At present, many scholars have researched adaptive regulation of streamflow change to mitigate the adverse effects of climate change and human activities on water resources systems (Zhang *et al.* 2021b), and the priority is to clarify the spatio-temporal distribution characteristics of streamflow and the driving factors; however, some existing studies have certain limitations, such as an inability to effectively reflect the streamflow characteristics of some sub-basins that are severely affected by direct human influences (i.e., water withdrawal from rivers and reservoir storage and discharge), and the differences in streamflow characteristics of different sub-basins within a basin, which may prevent water resource system managers from taking effective adaptive regulatory measures. Thus, the proposed spatio-temporal coupling analysis framework of streamflow change and its influencing factors is effective when trying to reflect the spatio-temporal characteristics of streamflow in sub-basins and fills the knowledge gap to a certain degree, which can consider the spatio-temporal synchronization and correlation of streamflow change.

5. CONCLUSIONS

This study aims to quantify the streamflow change and its influencing factors from a two-dimensional perspective in space and time with a spatio-temporal coupling analysis framework. The DRB (China) was taken as a case study and the key findings are as follows:

(1) The temporal variations of streamflow in the sub-basins of the basin are inconsistent (either increasing, decreasing, or constant). Also, the spatial patterns are time-variant, but all are clustered. That is, streamflow changes are found to be spatially and temporally synchronous and correlated.
(2) The natural streamflow change in the DRB during 1953–2013 is mainly affected by climate change–human activities, followed by climate change and human activities, accounting for a total area of 52.04, 24.90, and 23.06%, respectively.
(3) The vast majority of sub-basins within the basin with relatively large natural streamflow change during 1953–2013 are mainly driven by climate change (i.e., precipitation), which is related to the fact that direct impacts of human activities were not considered in this study.

FUNDING

This study was supported by the National Key R&D Program of China (Grant No. 2021YFC3090105); the Projects of the National Natural Science Foundation of China (Grant No. 52209032); the Natural Science Foundation of Jiangsu Province, China (Grant No. BK20200160); the Science and Technology Cooperation Support Project of Guizhou Province, China (Grant No. [2019]2890); and the Special Research Fund of Nanjing Hydraulic Research Institute (Grant No. Y120011).

DATA AVAILABILITY STATEMENT

Data cannot be made publicly available; readers should contact the corresponding author for details.

CONFLICT OF INTEREST

The authors declare there is no conflict.

REFERENCES

Bae, D.-H., Jung, I.-W. & Chang, H. 2008 Long-term trend of precipitation and runoff in Korean river basins. *Hydrological Processes* **22** (14), 2644–2656. https://doi.org/10.1002/hyp.6861.

Dariane, A. B. & Pouryafar, E. 2021 Quantifying and projection of the relative impacts of climate change and direct human activities on streamflow fluctuations. *Climatic Change* **165** (1–2). https://doi.org/10.1007/s10584-021-03060-w.

Dey, P. & Mishra, A. 2017 Separating the impacts of climate change and human activities on streamflow: a review of methodologies and critical assumptions. *Journal of Hydrology* **548**, 278–290. https://doi.org/10.1016/j.jhydrol.2017.03.014.

Gornik, M. 2020 Changing trends of river flows in the Upper Vistula Basin (East-Central Europe). *Acta Geophysica* **68** (2), 495–504. https://doi.org/10.1007/s11600-020-00400-9.

Johnson, N. C., Amaya, D. J., Ding, Q. H., Kosaka, Y., Tokinaga, H. & Xie, S. P. 2020 Multidecadal modulations of key metrics of global climate change. *Global and Planetary Change* **188**, 103149. https://doi.org/10.1016/j.gloplacha.2020.103149.

Lancaster, J. & Downes, B. J. 2004 Spatial point pattern analysis of available and exploited resources. *Ecography* **27** (1), 94–102. https://doi.org/10.1111/j.0906-7590.2004.03694.x.

Li, Z. & Quiring, S. M. 2021 Identifying the dominant drivers of hydrological change in the contiguous United States. *Water Resources Research* **57** (5), e2021WR029738. https://doi.org/10.1029/2021wr029738.

Li, Y., Chang, J., Luo, L., Wang, Y., Guo, A., Ma, F. & Fan, J. 2019 Spatiotemporal impacts of land use land cover changes on hydrology from the mechanism perspective using SWAT model with time-varying parameters. *Hydrology Research* **50** (1), 244–261. https://doi.org/10.2166/nh.2018.006.

Li, B., Shi, X., Lian, L., Chen, Y., Chen, Z. & Sun, X. 2020 Quantifying the effects of climate variability, direct and indirect land use change, and human activities on runoff. *Journal of Hydrology* **584**, 124684. https://doi.org/10.1016/j.jhydrol.2020.124684.

Ma, H. A., Yang, D. W., Tan, S. K., Gao, B. & Hu, Q. F. 2010 Impact of climate variability and human activity on streamflow decrease in the Miyun Reservoir catchment. *Journal of Hydrology* **389** (3–4), 317–324. https://doi.org/10.1016/j.jhydrol.2010.06.010.

McCabe, G. J. & Wolock, D. M. 2014 Spatial and temporal patterns in conterminous United States streamflow characteristics. *Geophysical Research Letters* **41** (19), 6889–6897. https://doi.org/10.1002/2014gl061980.

Meng, C., Zhang, H., Wang, Y., Wang, Y., Li, J. & Li, M. 2019 Contribution analysis of the spatial-temporal changes in streamflow in a typical elevation transitional watershed of southwest China over the past six decades. *Forests* **10** (6), 495. https://doi.org/10.3390/f10060495.

Pan, Z., Ruan, X., Qian, M., Hua, J., Shan, N. & Xu, J. 2018 Spatio-temporal variability of streamflow in the Huaihe River Basin, China: climate variability or human activities? *Hydrology Research* **49** (1), 177–193. https://doi.org/10.2166/nh.2017.155.

Wang, W., Zhang, Y. & Tang, Q. 2020 Impact assessment of climate change and human activities on streamflow signatures in the Yellow River Basin using the Budyko hypothesis and derived differential equation. *Journal of Hydrology* **591**, 125460. https://doi.org/10.1016/j.jhydrol.2020.125460.

Wang, M., Zhang, Y., Lu, Y., Gong, X. & Gao, L. 2021 Detection and attribution of reference evapotranspiration change (1951–2020) in the Upper Yangtze River Basin of China. *Journal of Water and Climate Change*. jwc2021011. https://doi.org/10.2166/wcc.2021.011.

Wilschut, L. I., Laudisoit, A., Hughes, N. K., Addink, E. A., de Jong, S. M., Heesterbeek, H. A. P., Reijniers, J., Eagle, S., Dubyanskiy, V. M. & Begon, M. 2015 Spatial distribution patterns of plague hosts: point pattern analysis of the burrows of great gerbils in Kazakhstan. *Journal of Biogeography* **42** (7), 1281–1292. https://doi.org/10.1111/jbi.12534.

Yang, Q., Scholz, M., Shao, J., Wang, G. & Liu, X. 2019 A generic framework to analyse the spatiotemporal variations of water quality data on a catchment scale. *Environmental Modelling & Software* **122**, 104071. https://doi.org/10.1016/j.envsoft.2017.11.003.

Yang, L., Zhao, G. J., Tian, P., Mu, X. M., Tian, X. J., Feng, J. H. & Bai, Y. P. 2022 Runoff changes in the major river basins of China and their responses to potential driving forces. *Journal of Hydrology* **607**, 127536. https://doi.org/10.1016/j.jhydrol.2022.127536.

Yuan, Z., Yan, D. H., Yang, Z. Y., Xu, J. J., Huo, J. J., Zhou, Y. L. & Zhang, C. 2018 Attribution assessment and projection of natural runoff change in the Yellow River Basin of China. *Mitigation and Adaptation Strategies for Global Change* **23** (1), 27–49. https://doi.org/10.1007/s11027-016-9727-7.

Zhai, H. J., Hu, B., Luo, X. Y., Qiu, L., Tang, W. J. & Jiang, M. 2016 Spatial and temporal changes in runoff and sediment loads of the Lancang River over the last 50 years. *Agricultural Water Management* **174**, 74–81. https://doi.org/10.1016/j.agwat.2016.03.011.

Zhang, K., Ruben, G. B., Li, X., Li, Z., Yu, Z., Xia, J. & Dong, Z. 2020 A comprehensive assessment framework for quantifying climatic and anthropogenic contributions to streamflow changes: a case study in a typical semi-arid North China basin. *Environmental Modelling & Software* **128**, 104704. https://doi.org/10.1016/j.envsoft.2020.104704.

Zhang, Y., Wu, X., Wu, S., Dai, J., Yu, L., Xue, W., Wang, F., Gao, A. & Xue, C. 2021a A framework for methodological options to assess climatic and anthropogenic influences on streamflow. *Frontiers in Environmental Science* **9**, 765227. https://doi.org/10.3389/fenvs.2021.765227.

Zhang, Y., Yu, L., Wu, S., Wu, X., Dai, J., Xue, W. & Yang, Q. 2021b A framework for adaptive control of multi-reservoir systems under changing environment. *Journal of Cleaner Production* **316**, 128304. https://doi.org/10.1016/j.jclepro.2021.128304.

Zhong, D., Dong, Z., Fu, G., Bian, J., Kong, F., Wang, W. & Zhao, Y. 2021 Trend and change points of streamflow in the Yellow River and their attributions. *Journal of Water and Climate Change* **12** (1), 136–151. https://doi.org/10.2166/wcc.2020.144.

First received 30 September 2022; accepted in revised form 11 April 2023. Available online 21 April 2023